JOC The Journal of Organic Chemistry

Article

pubs.acs.org/joc

Photocyclization and Photoaddition Reactions of Arylphenols via Intermediate Quinone Methides

Matthew Lukeman,*[,†] Hilary Simon,[†] Peter Wan,[‡] and Yu-Hsuan Wang*[,‡]

[†]Department of Chemistry, Acadia University, 6 University Ave., Wolfville, NS, B4P 2R6, Canada

[‡]Department of Chemistry, University of Victoria, Box 3065 Stn CSC, Victoria, BC, V8W 3V6, Canada

Supporting Information

ABSTRACT: A series of five benzannelated derivatives of 2-phenylphenol were prepared, and their photochemistry was investigated. Two of these (3-phenyl-2-naphthol, **10**, and 1-phenyl-2-naphthol, **11**) were photoinert. For 2-(1-naphthyl)phenol (**12**) and 1-(1-naphthyl)-2-naphthol (**13**), ESPT took place to either the 2′-position or the 7′-position of the naphthalene ring to give quinone methides (QMs) that underwent either reverse proton transfer (RPT) or electrocyclic ring closure to give dihydrobenzoxanthenes. The intermediate QMs for **12** and **13** were detected and characterized by laser flash photolysis. For 2-(9-phenanthryl)phenol (**14**), ESPT took place either to the 5′-position to give a QM that underwent quantitative electrocyclic ring closure to give the corresponding benzoxanthene or to the 10′-position to give a QM that underwent RPT. If the solution contained methanol, the QM produced on ESPT to the 10′-position in **14** could be trapped as the photoaddition product. The compounds studied in this work demonstrate three possible reactions of QMs produced following ESPT to aromatic carbon atoms: (1) reverse proton transfer (RPT) to regenerate starting material; (2) addition of hydroxylic solvents to give the photoaddition product; and (3) electrocyclic ring closure to give benzoxanthene derivatives.

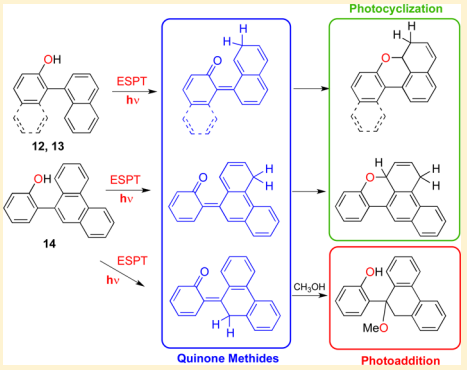

INTRODUCTION

Excited state intramolecular proton transfer (ESIPT) is an important and fundamental mechanism in which an acidic proton is transferred to a basic site within the same molecule on photoexcitation.[2] In most cases, the proton is transferred between two heteroatoms, and the reverse proton transfer (RPT) from the resultant tautomer to regenerate starting material is very fast. Such ESIPT processes are energy-wasting and have been exploited in the design of sunscreens and photostabilizers. Examples of ESIPT in which the proton acceptor is a carbon atom are comparatively rare, but are particularly interesting since these reactions generate quinone methide (QM) intermediates, for which the reverse proton transfer can be slow enough to allow other reaction pathways to compete.[3] In such cases, it is often possible to isolate new products that may be difficult to access thermally. For example, ESIPT to sp-hybridized alkynyl carbons gives rise to QMs that can be trapped by primary amines to give ketimine products.[3e]

We have investigated examples in which ESIPT takes place from a phenolic OH to carbon atoms of aromatic rings. For some compounds, including 2-phenylphenol[4] and 1-naphthol,[5] no new products are formed, and the primary evidence for the ESIPT process is the observation of deuterium exchange in recovered starting material, as shown in eq 1 for 2-phenylphenol. The deuterium exchange reaction of 2-phenylphenol was found to occur readily in aprotic solvents and in the solid state, suggesting that the proton is transferred directly from the OH to the basic carbon atom,[4] a mechanism that has been termed an "intrinsic" ESIPT reaction by Kasha.[6] Deuterium exchange quantum yields for 1-naphthol were found to strongly depend on the solvent D_2O concentration, suggesting that the proton transfer mechanism is best classified as a type of ESIPT termed by Kasha as a "proton relay tautomerization".[6] Such reactions are not truly "intramolecular"; however, since solvent molecules are required, so the term ESIPT is best reserved for those of the "intrinsic" type. We will use the more general term of excited state proton transfer (ESPT) to characterize reactions that are solvent-mediated.

We have shown that some examples of ESPT to aromatic carbon atoms do result in new product formation. For example, ESPT from the OH in anthracenylphenol **1** to the carbon atom at the 10′-position of the anthracene ring gives QM **2**, which can be trapped by water and alcohols to give the isolable photoaddition products **3** (eq 2).[7]

ESPT take places with good efficiency ($\Phi = 0.15$) in 1,1′-bi-2-naphthol (BINOL) from one of the hydroxyl groups to one of three different carbon atoms on the other ring system to give three QMs **4**–**6**.[8] Two of these (**4** and **5**) undergo RPT exclusively to regenerate starting material (labeled with deuterium when D_2O is present in the solvent mixture), while

Received: July 9, 2015
Published: October 23, 2015

DOI: 10.1021/acs.joc.5b01580
J. Org. Chem. 2015, 80, 11281−11293

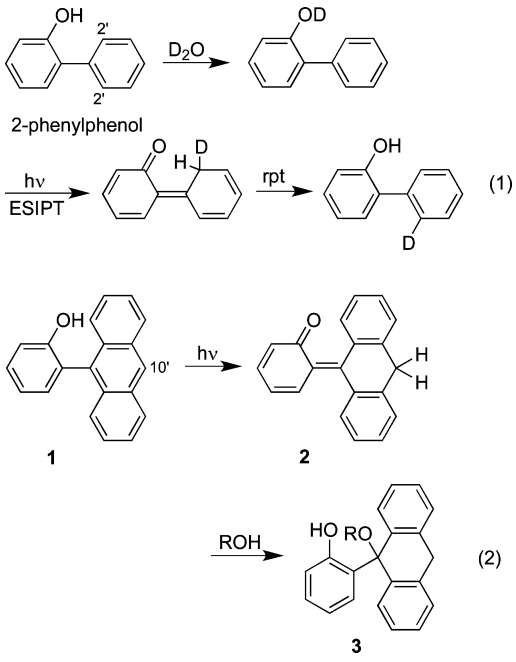

the third QM (**6**) undergoes electrocyclic ring closure to give dihydrobenzoxanthene **7** (Scheme 1). The ESPT−RPT reaction

Scheme 1

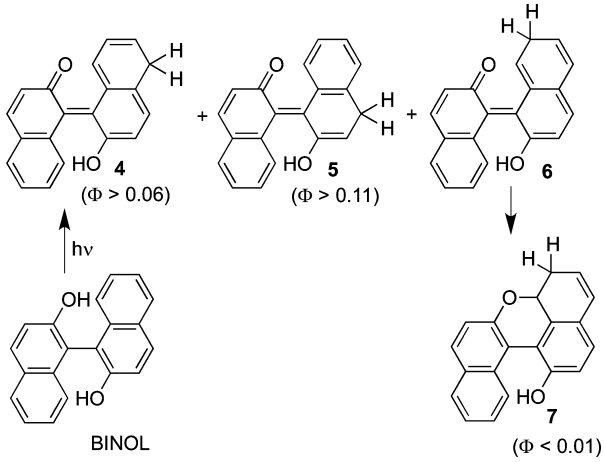

sequence causes racemization of enantiomerically pure samples of BINOL because of the planarity of the intermediate QMs **4** and **5**. While this discovery has important implications for catalysis, we were especially interested in the formation of **7**, since this represents a novel reaction pathway for photogenerated QMs. The formation of **7** from BINOL, however, is very inefficient (Φ < 0.01) and represents only a minor photochemical pathway.

In an effort to gain a more comprehensive understanding of ESPT to aromatic carbon atoms, we embarked on a study of the photochemistry of all possible monobenzannelated derivatives of 2-phenylphenol. We found that **8** undergoes ESIPT to the 2′-carbon of the attached phenyl ring, resulting in deuterium exchange when the solvent contains D_2O (eq 3), behavior that mirrors that of 2-phenylphenol (eq 1).[10] The quantum yield for deuterium incorporation for **8** was exceptionally high (Φ = 0.73), demonstrating that, at least for some phenols, ESIPT to aromatic carbon atoms is the dominant photochemical process. For **9**, we observed deuterium incorporation at the 1- and 3-positions of the naphthalene unit with a total quantum efficiency of Φ = 0.30 (eq 4), demonstrating that ESPT is a major photochemical pathway for this compound as well.[11]

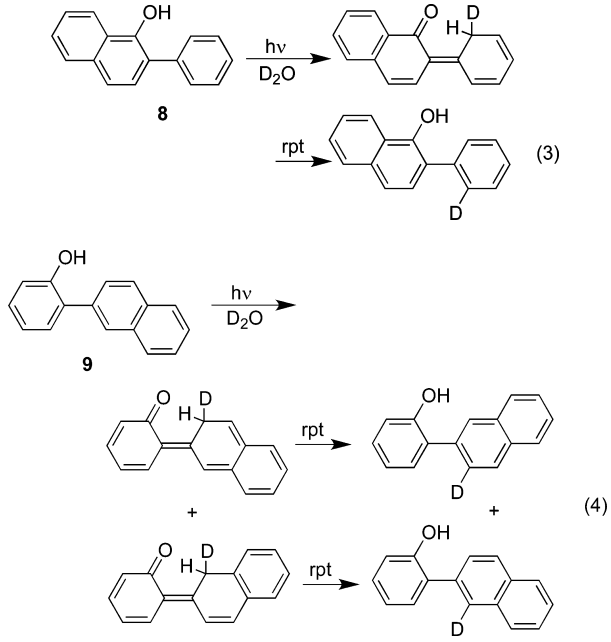

In the present work, we report our detailed study of the photochemistry of the remaining derivatives in the series of monobenzannelated derivatives of 2-phenylphenol, **10**−**12**. In addition, we report on the photochemistry of closely related dibenzannelated derivatives **13** and **14**. We demonstrate that three of these derivatives (**12**−**14**) undergo efficient ESPT processes, providing new examples of deuterium exchange, photoaddition, and photocyclization reactions.

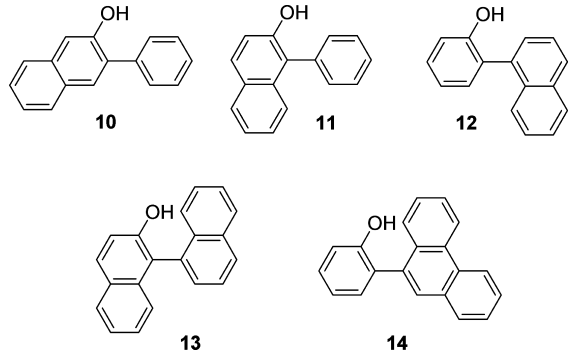

RESULTS AND DISCUSSION

Synthesis. Preparation of derivatives **10**−**14** was achieved in acceptable yield (19−84% over two steps) by the Suzuki coupling of the appropriate methoxyaryl boronic acid and aryl bromide to give methyl ethers **15**−**19**, followed by demethylation using BBr_3 (eq 5, Table S1). Aryl bromides and aryl boronic acids were commercially available, except for 3-bromo-2-naphthol, which was prepared according to the method of Niimi et al.[12] This synthetic scheme was attractive to us since it also provided methyl ethers **15**−**19**, whose photochemistry was also studied and compared with that of **10**−**14**.

$$\underset{\text{Ar}'\text{B(OH)}_2}{\overset{\text{MeOArBr}}{+}} \xrightarrow{\text{Pd(PPh}_3)_4} \underset{\textbf{15-19}}{\text{MeOAr-Ar}'} \xrightarrow{\text{BBr}_3} \underset{\textbf{10-14}}{\text{HOAr-Ar}'} \qquad (5)$$

DOI: 10.1021/acs.joc.5b01580
J. Org. Chem. 2015, 80, 11281−11293

Photochemical Experiments. The photochemistry of **10**–**14** was initially followed by UV–vis spectroscopy, with the expectation that photoaddition or photocyclization reactions might lead to changes in the absorption properties of the chromophores. Irradiation of derivatives **12**–**14** in deoxygenated aqueous acetonitrile (10%–50% water, v/v) did indeed lead to dramatic changes in the absorption spectra, and sharp isosbestic points were observed, indicating that the photoproducts are not undergoing secondary photochemistry under these conditions. Absorption spectra for **14** are shown in Figure 1; isosbestic points are visible

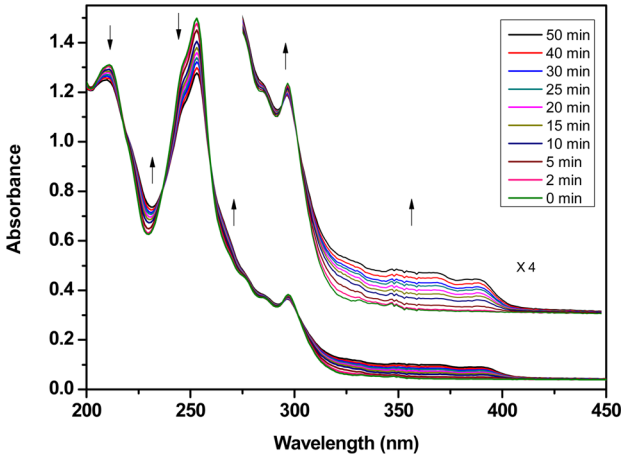

Figure 1. UV–vis spectra of **14** in 50% CH_3CN–H_2O (v/v) before and after irradiation in a Rayonet RPR 100 photoreactor at 300 nm (16 lamps). Irradiation times are indicated in the legend, and the arrows indicate whether the absorbance is increasing or decreasing in that wavelength range.

at 236, 260, 295, and 302 nm. A summary of absorption changes for **12**–**14** can be found in Table S3 in the Supporting Information.

There is a significant increase in absorbance in the 300–400 nm range, indicating that the photoproduct likely possesses more extended conjugation than **14**, as might be expected from a photocyclization reaction. It required much longer irradiation periods to bring about changes in the absorption spectra of **14** that were of a magnitude comparable to those for **12** and **13**, suggesting that the photoreaction leading to the absorption changes for **14** is much less efficient than that for **12** or **13**. No absorption changes were observed for solutions of phenols **10** or **11**, or methyl ethers of **12**–**14** (i.e., **17**–**19**) on irradiation.

In order to identify the photoproducts formed from irradiation of **12**–**14**, preparatory-scale photolyses were carried out in aqueous acetonitrile, and the photolysate was analyzed by TLC and NMR spectroscopy. TLC analysis of the photolysate produced on irradiation of a solution of **12** (deoxygenated 1:9 (v/v) H_2O–CH_3CN) indicated that, along with unreacted starting material, a single photoproduct had formed with a significantly higher R_f value than the starting phenol, indicating that the photoproduct is less polar than the starting material, likely lacking the phenolic OH. The photoproduct was isolated by preparatory TLC, and characterized by NMR spectroscopy. The NMR data were consistent with identification of this compound as dihydrobenzoxanthene **20** (eq 6). Treatment of **20** with Pd supported on carbon in oxygenated toluene resulted in >90% conversion to benzo[*k*,*l*]xanthene (eq 6). A similar preparatory-scale photolysis was carried out for **13** under the same conditions, and compound **21** was identified as the only photoproduct formed after it was isolated from the photolysate (eq 7). Both **20** and **21** are analogous in structure to **7** that is formed on irradiation of BINOL, indicating that this cyclization reaction might be general for hydroxybiaryls containing 1-naphthyl rings as proton-acceptors.

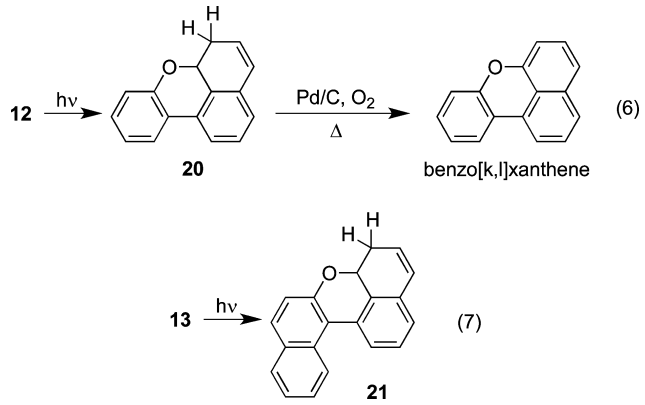

The photochemistry of **14** was investigated by carrying out preparatory-scale reactions in a variety of solvents. In aqueous acetonitrile, we envisioned two possible reactions: (1) photoaddition of water across the 9,10 phenanthrene double bond to give **22**, in analogy to the photochemistry of *o*-hydroxystyrene;[3b] and (2) photocyclization to give **23**, in analogy with the photochemistry of BINOL, **12** and **13** (Scheme 2).

Scheme 2

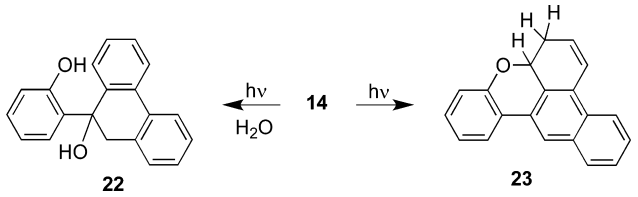

Irradiation of **14** (deoxygenated 1:1 (v/v) H_2O–CH_3CN) gave rise to a single photoproduct after chromatographic isolation from the photolysate that was identified as benzoxanthene **24** based on NMR and MS characterization. This product is similar in structure to **7**, **20**, and **21**, but represents a 2-electron oxidation (loss of H_2). We thought it likely that the first formed photoproduct was in actuality a dihydrobenzoxanthene such as **23** or **25**, which underwent oxidation to **24** during the workup and purification (eq 8). The photoreaction was repeated under the same conditions, but with the chromatography step omitted. NMR analysis indicated that the crude reaction mixture was primarily a mixture of starting material (**14**) and **24**, although, in addition to peaks arising from these, traces of a third product were detected that are consistent with expectations for **25**, supporting the assertion that **24** is formed from **25** after the initial photocyclization. It is not readily apparent why **25** is so much more oxygen sensitive than **20** and **21**, but perhaps the fact that the alkene group in **20** and **21** is conjugated with the phenyl ring imparts greater stability to these compounds. No evidence for the production of the hydrated photoproduct **22** was found in the photolysate NMR spectra.

DOI: 10.1021/acs.joc.5b01580
J. Org. Chem. 2015, 80, 11281–11293

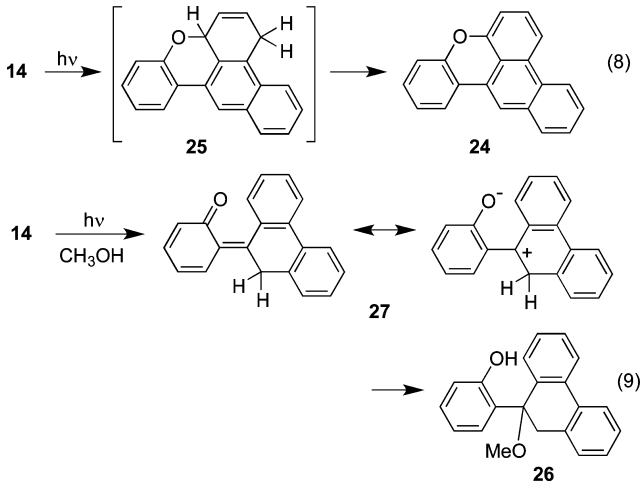

The photoreaction of **14** was repeated using various mixtures of water, methanol, and acetonitrile (Table S3, Supporting Information). When **14** was irradiated in neat methanol for 1 h, the sole product obtained was methyl ether **26** in 8% yield. This product likely arises from the initial formation of quinone methide **27**, followed by nucleophilic attack by methanol (eq 9). The analogous hydration product **22** was not observed in photoreactions conducted in aqueous acetonitrile, suggesting that **22** (if formed) is less stable than **26**, and dehydrates back to starting material. When **14** was irradiated in 1:4 water–methanol, the reaction to produce **26** became more efficient by a factor of approximately 6-fold, producing **26** in 51% yield. The enhancement in reaction efficiency observed when water is included in the solvent mixture is suggestive of a reaction mechanism involving an ESPT from the phenolic OH to the 10-carbon of the phenanthroline ring system to give QM **27**. In order to investigate the effect of excitation wavelength on the product yields, photolyses of **14** in 20% aqueous methanol were carried out using either UVA bulbs (λ_{max} = 350 nm) or UVB bulbs (λ_{max} = 300 nm) for 30 min. When UVA bulbs were used, **26** was obtained in 32% yield; however, the yield dropped to only 2% when the UVB bulbs were used. When UVB excitation is used, it is likely that the photoproduct **26** is absorbing the incoming light and undergoes photoelimination, reverting back to **14**. Since only the photoaddition product **26** was formed in aqueous methanol and only photocyclization product **24** was formed in aqueous acetonitrile, we decided to explore the photochemistry of **14** in aqueous methanol–acetonitrile mixtures in an attempt to promote a competition between the photoaddition and photocyclization pathways. Irradiation of **14** in a 2:1:5 mixture (v/v) of water–methanol–acetonitrile for 45 min led to formation of primarily photoaddition product **26** (13% yield) along with a smaller amount of **24** (<1% yield). When repeated for a much longer irradiation period (18 h), **26** and **24** were formed in 70% and 4% yields, respectively.

In order to determine the regiochemistry of the ESPT processes that operate for **12**–**14**, a series of photolyses was carried out in which the aqueous portion of the solvent mixture was replaced with D_2O. Photoproducts and recovered starting material were then monitored for deuterium incorporation (by ^{1}H NMR and MS) in order to identify the carbon atoms that act as proton acceptors. Irradiation of **12** (~10^{-3} M, 1:1 D_2O–CH_3CN, argon purged, 1 h) gave a mixture of **12** and **20**, along with a small amount of other unidentified photoproducts that were not formed when the solvent mixture was 1:9 H_2O–CH_3CN. **12** and **20** present in the photolysate were separated by preparatory TLC and analyzed separately by ^{1}H NMR spectroscopy. The sample of recovered **12** thus obtained showed a 45% decrease in the integrated area of the peak assigned to the proton at the 2′-position of the naphthalene ring at 7.90 ppm, indicating a 55:45 ratio of **12**:**12**-2′*D* (eq 10).

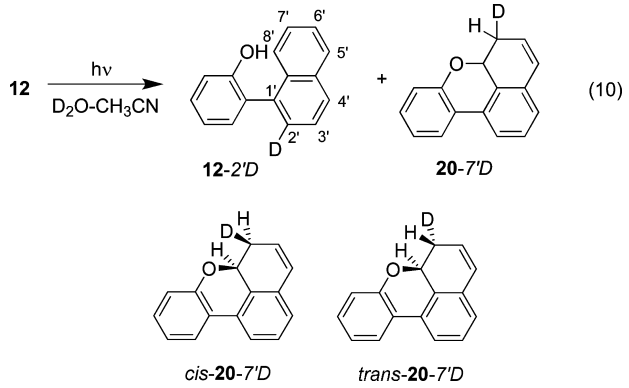

The decrease in area is accompanied by the transformation of the peak at 7.54 ppm (assigned to the adjacent 3′-position) from a well-defined doublet of doublets to a broad doublet, with no loss of total peak area (see the Supporting Information). The change in this peak is consistent with the reduced coupling that would occur on exchange of the adjacent hydrogen with deuterium. Photoproduct **20** isolated from the same run showed exactly 50% deuterium exchange at the methylene (7′-) position (to give **20**-7′*D*) (eq 10), as evidenced by the 50% reduction in peak area at δ3.43 ppm in the ^{1}H NMR spectrum (Figure 2),

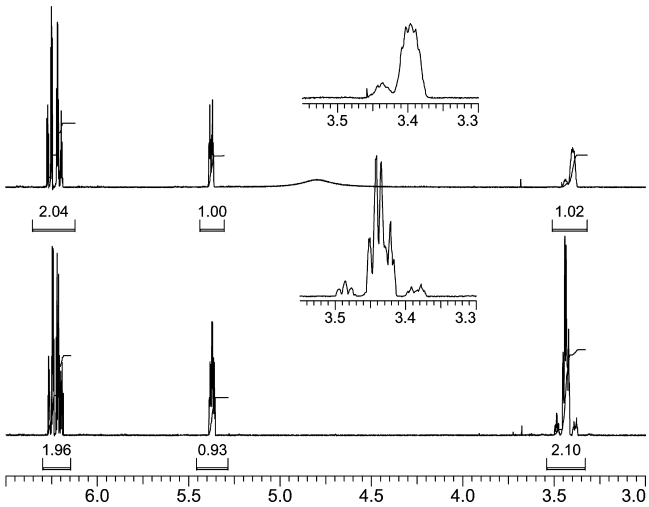

Figure 2. 500 MHz ^{1}H NMR spectra of **20** produced by irradiation of **12** in 1:9 H_2O–CH_3CN (bottom) and in 1:9 D_2O–CH_3CN (top) solutions, showing the 50% decrease in peak integration of the signal at 3.4 ppm.

suggesting that one of the methylene hydrogen atoms in **20** comes from either the phenol OH (or OD) or solvent H_2O (D_2O). The methylene signal for **20**-7′*D* actually consists of two peaks, one centered at 3.40 ppm, and the second centered at 3.44 ppm, and these peaks are present in a 3:1 ratio (by area). These separate signals might arise from the two possible diastereomers of **20**-7′*D*: one in which the methylene deuterium is *cis* to the ether oxygen (*cis*-**20**-7′*D*), and one in which the methylene deuterium is *trans* to the ether oxygen (*trans*-**20**-7′*D*).

DOI: 10.1021/acs.joc.5b01580
J. Org. Chem. 2015, 80, 11281–11293

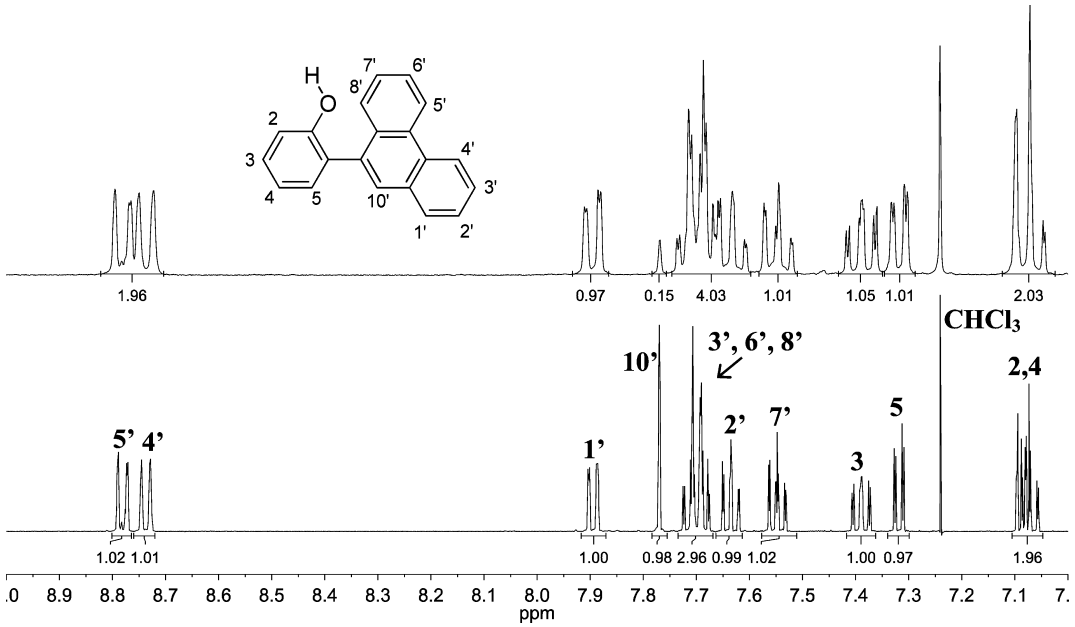

Figure 3. 500 MHz ^{1}H NMR spectra of **14** before (bottom) and after (top) irradiation in 1:1 D_2O−CH_3CN solution, showing ∼85% decrease in the singlet at 7.78 ppm, assigned to the 10′-hydrogen. Relative integrations are given below the curve.

Similar photolyses of **13** in solutions in which the aqueous portion was replaced with D_2O led to formation of **21**-7′*D* (eq 11). Exactly one deuterium atom is incorporated at the methylene position in **21**-7′*D*, whether the reaction is taken to low or high conversion, ruling out a mechanism in which the deuterium exchange occurs in a separate process from formation of **21**. The methylene signal in this case appears as only one peak, suggesting that only a single diastereomer is formed (Figure S1, Supporting Information). Starting material isolated from these photolyses showed deuterium incorporation at the 2′-position, the extent of which rose steadily as the reaction was taken to higher conversion; irradiation for 10 or 30 min led to a 60% or 85% decrease in the integrated area of the peak at 8.02 ppm that is assigned to the aromatic hydrogen at the 2′-position, and a 5% or 10% decrease in the integrated area of the peak at 7.97 ppm that is assigned to the aromatic hydrogen at the 8′-position. Accompanying these changes is the conversion of the doublet of doublets at 7.65 ppm assigned to the 3′-position to a broad doublet, due to diminished coupling with deuterium at the 2′-position.

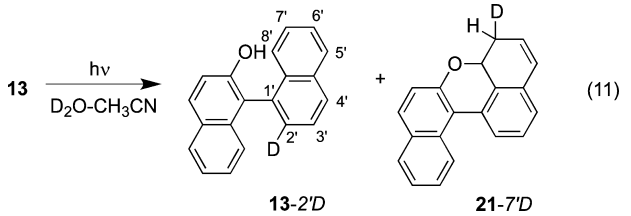

(11)

Irradiation of solutions of **10** and **11** containing D_2O for extended periods of time (2−20 h) yielded only starting material with no deuterium incorporation, indicating that ESPT processes to aromatic carbons are not important pathways for these phenols. The methyl ether analogues (**17**−**19**) also did not show deuterium incorporation when irradiated in D_2O solution, implying that the OH moiety in **12** and **13** is required for their photochemistry.

The photochemistry of **14** was also explored in acetonitrile solutions containing D_2O. Irradiation of **14** (∼10^{-3} M, 1:1 D_2O−CH_3CN, argon purged, 3 h) produced a mixture of **24** and **14**. The products were chromatographically separated and analyzed by ^{1}H NMR spectroscopy to assess for deuterium incorporation. The recovered starting material showed an 85% reduction in the peak area of the singlet at 7.69 ppm assigned to the hydrogen at the 10′-position on the phenanthrene ring system (Figure 3), indicating that photolysis led to extensive conversion to **14**-10′*D* (Scheme 3). The likely reason for the deuterium exchange is initial ESIPT from the phenolic OD to the 10′-carbon to give **27**-10′*D*, which then either undergoes RPT to give **14**-10′*D* directly or is first hydrated by the solvent to give **22**-10′*D*, which subsequently dehydrates to give **14**-10′*D* (Scheme 3). The cyclized photoproduct **24** isolated from the same run showed significant deuterium incorporation in two positions. The peak area of the singlet at 7.71 ppm assigned to the 10′-hydrogen was reduced by approximately 65%, indicating formation of **24**-10′*D*, which probably arises from cyclization of **14**-10′*D* that was previously formed by the process depicted in Scheme 3.

In addition, the peak area of the doublet at 8.10 ppm assigned to the hydrogen on the 5′-carbon was reduced by 58%, indicating formation of **24**-5′*D*, suggesting that an ESPT from the phenolic OD of **14** takes place to the 5′-carbon to form QM **28**-5′*D*, which then quantitatively cyclizes to **25**-5′*D*, which gives **24**-5′*D* after air oxidation (Scheme 3). The quantitative nature of the cyclization is suggested by the fact that no deuterium exchange was observed at the 5′-position in recovered starting material. Because QM **28**-5′*D* and **25**-5′*D* should both contain exactly one deuterium and one hydrogen atom on the methylene carbon, the observed deuterium exchange of 58% at the 5′-position of **24**-5′*D* indicates that the oxidation step exhibits a kinetic isotope effect of k_H/k_D = 58%/42%, or 1.4. In addition to **24**-5′*D* and **24**-10′*D*, formation of dideuterated **24**-5′,10′*D* is also expected in higher conversion runs, although the dideuterated product is indistinguishable from the monodeuterated products by ^{1}H NMR spectroscopy.

A series of photolyses of **12**−**14** were carried out in which the concentration of D_2O (in CH_3CN) was systematically altered so that the role of water in the photoreaction could be better understood. For **12** and **13**, the efficiency of product formation is

DOI: 10.1021/acs.joc.5b01580
J. Org. Chem. 2015, 80, 11281−11293

Scheme 3

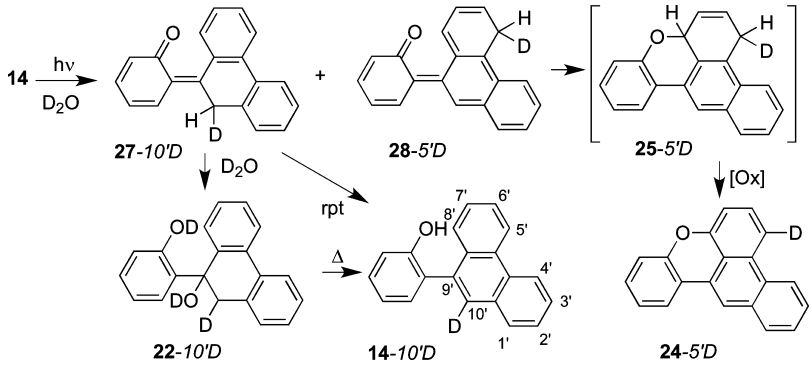

highly dependent on the concentration of D_2O present in solution.[1] ESPT reaction efficiency is minimal at low water concentrations, but rises steadily as more D_2O is added, reaching a maximum at 5 M D_2O (10% (v/v)). The water dependence indicates that the reactions are not examples of intrinsic ESIPT, but are best explained as arising from a water-mediated ESPT. A similar water (D_2O) dependence study was carried out for the ESIPT reaction of **14** to form **14**-10′*D*. Solutions of **14** containing varying amounts of D_2O in CH_3CN were irradiated, and the photolysate was analyzed by ^1H NMR spectroscopy (Figure 4).

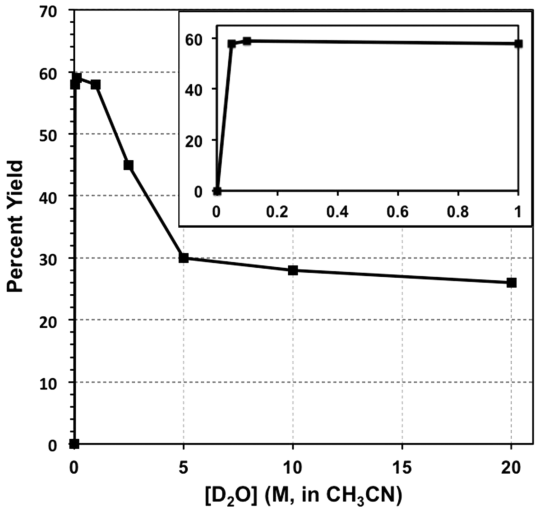

Figure 4. Plot showing % yield of **14**-10′*D* formed on irradiation of **14** solutions in CH_3CN containing varying concentrations of D_2O. The inset is an expansion of the 0−1 M region of the plot.

The yield of **14**-10′*D* is only weakly dependent on D_2O concentration in the 5−20 M range, but increases dramatically as the D_2O concentration is reduced below 5 M, so that, at 0.5 M D_2O, the yield of **14**-10′*D* is twice as high as when the D_2O concentration is higher than 5 M. The ESIPT reaction yield remains high until very small water concentrations are reached (<0.05 M), and at such low concentrations, it is difficult to ensure isotopic purity due to contamination from trace amounts of H_2O present in the CH_3CN and/or on the glassware. The ESPT reaction for **14** clearly does not require significant quantities of water (or D_2O), suggesting that the reaction is an intrinsic ESIPT. Intrinsic ESIPT reactions typically require that the acidic OH and basic carbon atom be close to each other in space and share a ground state hydrogen-bonding interaction, which is certainly possible for **14** and is consistent with results we recently reported for the related 9′-(2,5-dihydroxyphenyl)-phenanthrene.[9a] The rise in efficiency on moving from 5 M D_2O to 0.5 M D_2O might be the result of a competing ESPT reaction from the phenol OH of **14** to solvent water, which increases in efficiency as the water concentration in the solvent increases. At low water concentrations, this pathway becomes less important, allowing for maximal ESIPT efficiency. Also, water (or D_2O) present in the solvent would be expected to hydrogen bond with the phenolic OH, thereby potentially interfering with any intramolecular hydrogen-bonding interaction with the π-system of the phenanthrene ring.[13]

Quantum yields for both photocyclization and deuterium incorporation (in 10% D_2O−CH_3CN) were determined for **12**−**14**, using the deuterium exchange of 2-phenylphenol in the same solvent (Φ = 0.042) as a secondary reference standard.[4] The quantum yields appear in Table 1, where Φ_D refers to the quantum yield for deuterium incorporation in starting material, and Φ_{cyc} refers to the quantum yield for formation of the cyclized benzoxanthenes **20**, **21**, and **24**. The quantum yield for the photoaddition of methanol to **14** was not determined. However, this addition and the deuterium exchange reaction at the 10′-position are assumed to share a common intermediate **27**, and thus, these processes should have the same quantum yield for the primary photochemical step (ESPT).

Table 1. Quantum Yields for the Formation of Deuterated Starting Material (Φ_D) and Cyclized Photoproduct (Φ_{cyc}) for 10−14 D_2O−CH_3CN Mixtures[d]

compound	Φ_D	Φ_{cyc}
10	0[a]	0[a]
11	0[a]	0[a]
12	0.14[a]	0.20[a]
13	0.11[a]	0.11[a]
14	0.18[b]	0.005[b]
	0.36[c]	<0.01[c]

[a]In 1:9 (v/v) D_2O−CH_3CN solution. [b]In 1:1 (v/v) D_2O−CH_3CN solution. [c]In 1:99 (v/v) D_2O−CH_3CN solution. [d]Estimated errors are ±10% of quoted value.

Fluorescence Measurements. Excitation of **11** (λ_{ex} = 334 nm) in neat CH_3CN gives strong fluorescence emission with a maximum at 353 nm (Table 2). The Stokes shift is small (19 nm), suggesting that two aryl rings do not twist significantly toward planarity on excitation. Both the absorption and the emission maxima of $\mathbf{11}^-$ (formed by dissolving **11** in a 1:1 mixture of 0.01 M NaOH and CH_3CN) are red-shifted relative to **11** (Table 2).

DOI: 10.1021/acs.joc.5b01580
J. Org. Chem. 2015, 80, 11281−11293

Table 2. Photophysical Data for 10−14[d]

compound	λ_{ex} (nm)	λ_{em}	τ_S (ns)	Φ_F	k_F (s^{-1})
11	334[a]	353[a]	8.5[a]	0.19	2.2×10^7
11$^-$	368[a]	445[b]			
12	293[a]	355[a]	3.0[a]		
12$^-$		540[c]			
13	334[a]	356[a]	3.9[a]		
13$^-$	370[b]	550[b]			
14	296	353, 370, 390 (sh)	27.5[a]	0.22[a]	8.0×10^6
			17.4[c]	0.10[c]	5.7×10^6

[a]In neat CH_3CN. [b]In 1:1 water−CH_3CN, pH 12. [c]In 4:1 water−CH_3CN. [d]Estimated errors are ±10% of quoted value.

Excitation of **12** (λ_{ex} = 293 nm) in neat CH_3CN (argon purged) gave a strong emission at 355 nm that exhibited a much larger Stokes shift (62 nm) than that observed for **11**, indicating that significant twisting about the biaryl bond toward planarity occurs on excitation to S_1. If the excited state of **12*** is nearly planar, this should allow for much stronger charge transfer from the phenolic ring to the naphthyl ring in the excited state due to the better $\pi-\pi$ overlap between the rings, which is thought to be a requirement for efficient ESIPT reactions in biaryls. Similarly, the lack of planarity of **11***, as suggested by the small Stokes shift, may explain the fact that this compound does not undergo ESIPT reactions. For **12**, the fluorescence emission intensity was very sensitive to the amount of water present in the solution. Addition of small amounts (~1 M H_2O) to the acetonitrile solvent caused an initial red-shifting of the emission band to 360 nm, along with a modest increase in intensity. These effects are associated with solvation by water. Addition of larger amounts of water led to a dramatic quenching of the fluorescence emission until ~10 M water was reached, at which point addition of more water did not lead to significant further quenching. The quenching of the fluorescence emission of **12** with added water correlates well with the increase in ESPT reaction efficiency on addition of water. We propose that the fluorescence quenching with added water (up to 10%) is a result of the increasing competition from ESPT of **12** as water is added. This correlation is strong evidence for reaction of **12** from S_1 and not T_1. The further fluorescence quenching (from 10% up to 40% water content) is likely a result of increasing competition from ESPT to the bulk solvent. Addition of larger amounts of water led to the growth of a new weak emission band at 540 nm, which we assign to fluorescence from the phenolate **12**$^-$ that would form on ESPT to the solvent water. Addition of greater amounts of water (from 40% up to 100%, data not shown) led to a red-shifting of the fluorescence emission maximum from 360 to 386 nm, an effect that may simply result from changes of the overall polarity of the solvent.

Excitation of **13** in neat CH_3CN (λ_{ex} = 334 nm) gave strong, broad, and structureless fluorescence emission at 356 nm (Figure S3, Supporting Information). The Stokes shift for **13** (22 nm) is smaller than that of **12**, indicating that rotation toward planarity is not achieved to the same extent for the former, likely as a consequence of the additional steric bulk present in **13**. Excitation of **13**$^-$ (formed by dissolving **13** in a 1:1 mixture of 0.01 M NaOH and CH_3CN) at λ 370 nm gave weak fluorescence emission at λ 550 nm. The position of this band is similar to that of **12**$^-$, and the Stokes shift is very large (180 nm), suggesting that twisting to planarity is much more facile for **13**$^-$ than for **13**. Addition of small amounts of water led to very efficient quenching of the 356 nm fluorescence band for **13**, with over 80% quenching observed at less than 3 M H_2O (Figure S3). A Stern−Volmer quenching plot was constructed and appears as the inset in Figure S3. The quenching data is nonlinear, and fit best to $I_0/I = 1 + K_{SV}[H_2O]^{1.7}$. We attribute this quenching to competition from the ESPT process that is enabled by the added water. Along with the quenching of the 356 nm band, a very weak band is observed to grow in at ~550 nm, corresponding to emission from the naphtholate, indicating that adiabatic ESPT from the hydroxyl group to solvent (water) to form **13**$^-$* can take place at high water concentrations. There may be a contribution to the observed quenching due to a simple solvent polarity change as well, but such a contribution is expected to be small at water concentrations less than 3 M, since changes due to solvent polarity were not seen for **12** until concentrations of over 20 M were reached.

Excitation of **14** in neat CH_3CN (λ_{ex} = 300 nm) resulted in structured fluorescence emission with maxima at 353 and 370 nm. Addition of water to the acetonitrile solvent lead to an increase in fluorescence emission intensity from **14**, and when a water concentration of 27.8 M was reached, the fluorescence emission intensity had more than doubled. Addition of more water beyond 27.8 M reduced the emission intensity, and at water concentrations greater than 35 M H_2O, the emission intensity was once again lower than that in pure acetonitrile. The product studies revealed that the ESIPT reactions of **14** were most efficient at very low water concentrations (<5 M D_2O). Thus, the low fluorescence emission in acetonitrile solutions containing little or no water can be explained by the fact that the ESIPT processes that compete with fluorescence at these solvent compositions are maximally efficient. Fluorescence lifetimes (τ_F) were measured in neat CH_3CN and in 4:1 H_2O-CH_3CN solutions and were found to be 27.5 and 17.4 ns, respectively (Table 2). The fluorescence quantum yields (Φ_F) were also measured in neat CH_3CN and in 4:1 H_2O-CH_3CN solutions and were found to be 0.22 and 0.10, respectively. The reduction in fluorescence quantum yields and fluorescence lifetimes in aqueous acetonitrile indicates that dynamic quenching of S_1 by water takes place, which we interpret as being due to ESPT to solvent. Using these values, the fluorescence rate constants (k_F) were determined using eq 12 and appear in Table 2.

$$k_F = \Phi_F \times (1/\tau_F) \tag{12}$$

Laser Flash Photolysis. Nanosecond laser flash photolysis (LFP) was employed in an attempt to characterize the transient species formed on ESIPT of **12**−**14**, with the primary aim of detecting QM intermediates that would form on ESIPT to an aromatic carbon position. Related *o*-naphthoquinone methides (NQM) have been reported by the Popik[14a,b] and Freccero[14c,d] groups, although these are formed from photoelimination of benzylic alcohols or quarternary ammonium salts, rather than ESIPT to carbon atoms. Several of these NQMs were detected by

DOI: 10.1021/acs.joc.5b01580
J. Org. Chem. 2015, 80, 11281−11293

LFP and showed an absorption band at around 360 nm. However, these NQMs are confined to a single naphthalene unit and are not biaryl quinone methides like those expected from **12**–**14**.

LFP of **12** in neat CH_3CN (N_2 purged) gave a weak transient that absorbed between 320 and 550 nm with a maximum at 440 nm and a lifetime of 800 ns. Saturation of the solution with oxygen led to quenching of the transient, leading us to assign this transient to the triplet state of **12**. LFP of **12** in 1:9 H_2O–CH_3CN (N_2 or O_2 purged) gave a number of transients (Figure 5). A band was observed at 490 nm with a lifetime

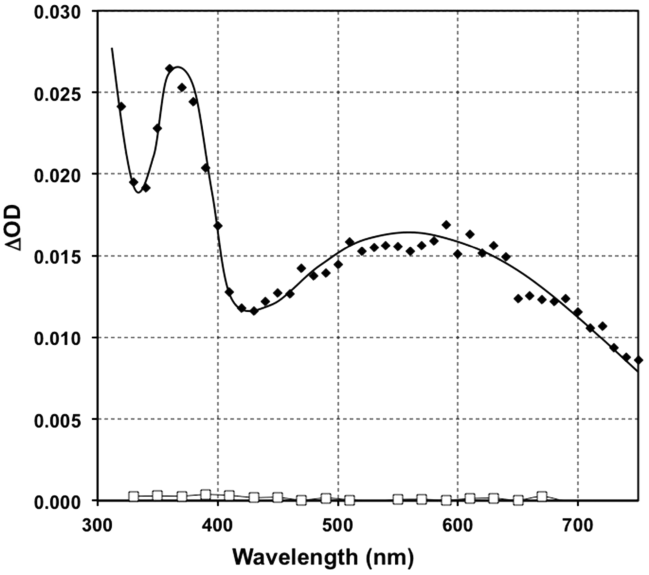

Figure 5. Transient absorption spectra observed on LFP of **12** in 1:9 CH_3CN (black diamonds) and in neat CH_3CN (white squares) (O_2 purged, λ_{ex} = 308 nm). Absorption data were taken immediately after the laser pulse.

of 800 ns that was quenched on saturation of the solution with oxygen. This transient is similar to that observed in neat CH_3CN and is assigned to the triplet state. In addition to the triplet signal, a second transient absorption was observed with maxima at 360 and 560 nm. Both maxima showed a decay that fit best to a double exponential function with lifetimes of 3 and 400 μs, indicating the presence of two species. Neither lifetime was reduced by the presence of oxygen, consistent with the assignment of these signals to QM intermediates. ESPT in **12** from the OH to the 2′-position or 7′-position would give **28** and **29**, respectively (eq 13).

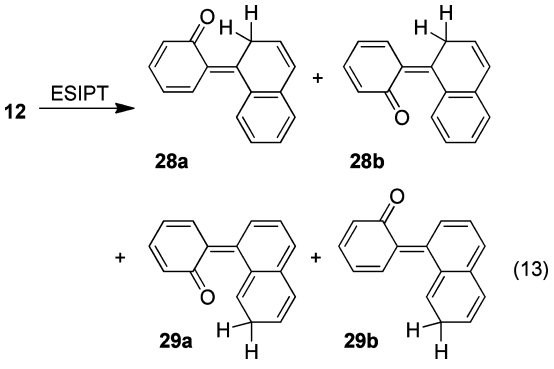

Both of these QM intermediates can conceivably be generated in either of two isomeric forms, **28a** and **28b**, and **29a** and **29b**. Isomer **29a** does not undergo reverse proton transfer, as evidenced by the lack of deuterium incorporation at the 7′-position, so electrocyclic ring closure must be much faster than reverse proton transfer. For this reason, we expect **29a** to be short-lived. Isomer **29b** is probably not formed at all, since it cannot cyclize, and we saw no isotope exchange following irradiation in D_2O. We, therefore, provisionally assign the two transients observed on LFP of **12** in aqueous solution to be due to two of the QMs **28a**, **28b**, and **29a**. We do not feel that more definitive assignments can be made with the information at hand.

In analogy to the photochemistry of **12**, ESPT to the 2′- or 7′-position of **13** would give QMs **30a**, **30b**, **31a**, and **31b** (eq 14). As was also the case for **12**, starting material that was isolated from irradiations of **13** in D_2O solution showed no measurable deuterium incorporation at the 7′-position, indicating that QM **31a** exclusively undergoes ring closure, and that QM **31b** is not formed. Electrocyclic ring closure for **30a** is not possible, and is not favorable for **30b** because this process would reduce the aromaticity of the system. Instead, QMs **30a** and **30b** undergo reverse proton transfer (tautomerization). LFP of **13** in 1:9 H_2O–CH_3CN solution (oxygen purged) gave rise to a transient spectrum that showed strong absorption across the entire visible region that tailed beyond 800 nm (Figure 6). A biphasic decay was observed at all wavelengths, with a long-lived ($\tau \sim 580$ μs) and a shorter-lived ($\tau \sim 120$ μs) component, indicating the presence of two decaying species. Both of these lifetimes are rather long, and neither can be assigned to **31a**, since it is unlikely that **31a** would persist for 120 μs and still undergo quantitative cyclization with no RPT. On this basis, we provisionally assign the two transients to **30a** and **30b**.

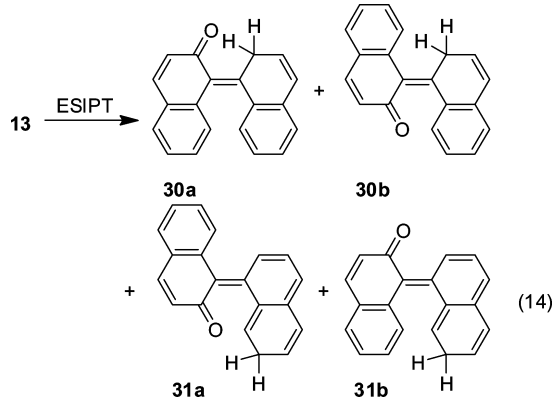

LFP was also carried out on **14** in hopes of detecting QMs **27** or **28**. LFP of **14** in neat CH_3CN (nitrogen purged) gave a transient absorption with λ_{max} = 430 nm and a lifetime of 4.9 μs. When the solution was purged with oxygen, the lifetime of the transient was reduced to 56 ns, consistent with this transient being the triplet–triplet absorption of **14**. Since the ESIPT (to the 10′-position) has been shown to be maximally efficient in CH_3CN containing little to no water (Figure 4), the absence of additional observable signals might indicate that QM **25** (*cis* or *trans*) has a lifetime shorter than 20 ns, the time resolution of the instrument. The analogous QM produced by ESIPT in 2-phenylphenol was also undetectable by nanosecond LFP, although it has been recently detected in femtosecond transient absorption experiments.[15] LFP experiments were also conducted on **14** in a 1:1 mixture of water and acetonitrile under both nitrogen- and oxygen-saturated conditions; however, no signals in addition to the triplet were observed under these conditions.

DOI: 10.1021/acs.joc.5b01580
J. Org. Chem. 2015, 80, 11281–11293

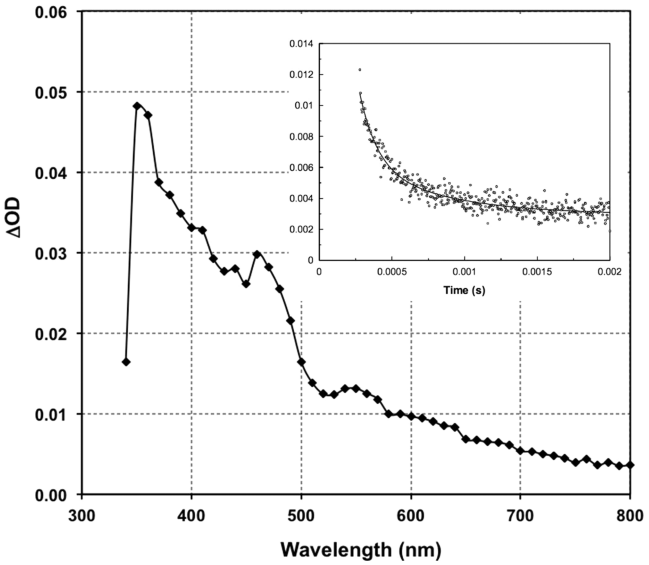

Figure 6. Transient absorption spectra observed on LFP of **13** in 1:9 CH_3CN (O_2 purged, λ_{ex} = 308 nm). Absorption data were taken immediately after the laser pulse. Inset: Biphasic decay of the absorption at 550 nm observed on LFP of **13** in 1:9 CH_3CN (O_2 purged, λ_{ex} = 308 nm). Line drawn is least-squares fit to the equation $\Delta OD = A + Be^{-(k1)t} + Ce^{-(k2)t}$, and gives τ_1 = 580 μs and τ_2 = 120 μs.

Mechanism. The photochemical pathways available to **12** are summarized in Scheme 4. Following excitation to S_1, ESPT can

Scheme 4

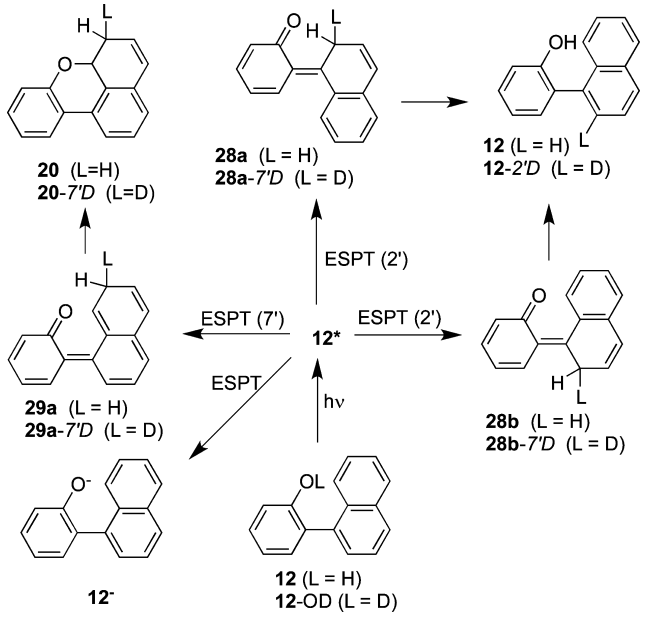

proceed from the phenol OH to the 7′-position of the naphthalene ring to give QM **29a**, provided a sufficient amount of water is present to mediate the proton transfer (optimally ~5 M). QM **29a** quantitatively undergoes 6π-electrocyclic ring closure to give dihydrobenzoxanthene **20** and does so at a rate that is sufficiently fast so that RPT cannot compete. When the reaction is carried out in D_2O solution, excited state deuterium transfer (ESDT) instead gives **29a**-7′*D*, which cyclizes to **20**-7′*D*. ^{1}H NMR spectroscopy of **20**-7′*D* indicates the formation of a 3:1 mixture of *cis* and *trans* isomers of **20**-7′*D*. If **29a**-7′*D* is formed as a discrete intermediate prior to cyclization, a *cis*/*trans* ratio close to 1:1 would be expected, since **29a** is planar and should cyclize in either direction with equivalent likelihood, excepting any isotope effect imparted by the presence of deuterium, which would be only secondary. One way to explain the 3:1 isomer ratio would be to invoke a mechanism in which proton transfer occurs concurrently with rotation of the rings toward planarity, and cyclization takes place before a planar QM can be formed, as depicted in Scheme 5. If **20**-7′*D* is formed via this concerted mechanism 50% of the time, and the other 50% of the time, the rotation to 0° takes place to give **29a**-7′*D*, one would expect a product ratio of approximately 3:1, as observed. ESPT can also take place to the 2′-position to give QM **28a** and/or **28b**, both of which quantitatively undergo reverse proton transfer to regenerate starting material (or deuterium-labeled starting material **12**-2′*D* when carried out in D_2O solution).

The photochemistry of **13** is very similar to that of **12** presented in Scheme 4. ESIPT to the 2′- and 7′-positions gives QMs **30a**, **30b**, and **31a**. QM **31a** undergoes quantitative cyclization to **21**. When carried out in D_2O solution, **21**-7′*D* is instead formed, and ^{1}H NMR spectroscopy does not show evidence for the presence of more than one diastereomer of **21**-7′*D*, which might mean that a concerted mechanism takes place that is similar to that in Scheme 5 for **12**, but occurs quantitatively for **13**, which can be rationalized by the additional steric bulk present for **13**, which would hinder the rotation to planarity necessary to produce **31a**. QMs **30a** and **30b** revert to starting material via reverse proton transfer to give **10**, labeled with deuterium at the 2′-position when carried out in D_2O solution.

Irradiation of **14** in acetonitrile, alcohols, or aqueous acetonitrile results in either ESPT from the phenolic OH to the 5′-carbon or ESIPT to the 10′-carbon of the phenanthrene ring system, producing QMs **28** or **27**, respectively (Scheme 6). QM **28** undergoes quantitative cyclization to **25**, which gives **24** after oxidation by air. QM **27** can be trapped by methanol to give the photoaddition product **26**. In aqueous acetonitrile not containing methanol, **27** will revert back to **14**, possibly via the unstable hydration product **22**. Similar reaction pathways were shown to be available to related phenanthrene systems.[9a]

The inert derivatives **10** and **11** are structurally similar in that they both possess the 2-naphthol unit and an attached phenyl ring—which is apparently an unfavorable combination for ESIPT reactions. The example of **8** shows that ESPT can take place efficiently from a 1-naphthol OH to an attached phenyl ring.[10] The lower reactivity of 2-naphthols **10** and **11** relative to 1-naphthol **8** might partly result from the fact that the phenolic OH in 1-naphthol is more acidic (pK_a^* = 0.4) than the OH in 2-naphthol in S_1 (pK_a^* = 2.8).[16] However, the examples of BINOL and **13** show that the 2-naphthol unit can function as the ESIPT "donor" ring system. In addition, ESIPT giving QM intermediates has been demonstrated by the Popik group in several 3-substituted 2-naphthols with moderately efficient quantum yields ($\Phi \sim 0.20$), indicating that charge transfer from 2-naphthol can take place from the OH to substituents attached to the 3-position.[14a,b,17] In these examples, however, ESIPT may be facilitated by the fact that the proton-accepting groups are more basic in S_1 than the simple phenyl rings present in **10** and **11**. Perhaps the lack of reactivity of **10** and **11** is a combined effect of the phenolic OH being not quite acidic enough, and the phenyl ring being not quite basic enough. It is important to note that all examples of ESPT discovered in this work occur from the phenol OH to the aromatic system not

DOI: 10.1021/acs.joc.5b01580
J. Org. Chem. 2015, 80, 11281−11293

Scheme 5

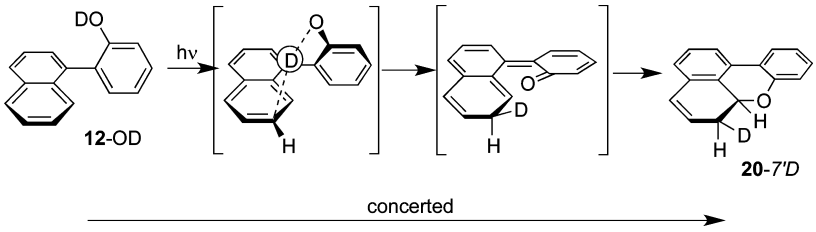

Scheme 6

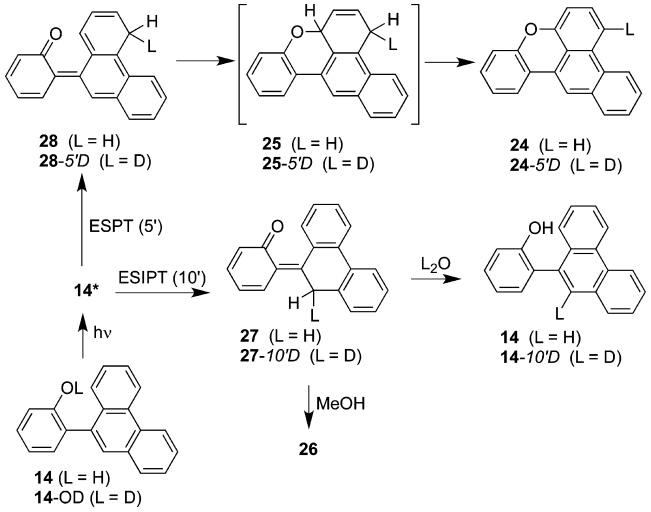

containing the OH. This fact indicates that **12**−**14** have strongly polarized singlet excited states that result from significant charge transfer from the phenolic ring (which is the electron-rich ring in S_0) to the nonphenolic ring, and that all proton transfers to aromatic carbon atoms take place on the excited state energy surface.

CONCLUSIONS

Our investigation into the photochemistry of substituted phenyl phenols continues to unearth interesting new reaction types and provide mechanistic insights into the more general mechanistic class of ESPT to aromatic carbon atoms. The compounds studied in this work show three distinct reaction types: (1) formation of QMs that undergo RPT to regenerate starting material (with possible deuterium incorporation); (2) formation of QMs that can be trapped by solvent to give addition products; and (3) formation of QMs that undergo electrocyclic ring closure to give benzoxanthene derivatives.

EXPERIMENTAL SECTION

General. Acetonitrile used in all experiments was HPLC or spec. grade and was distilled over CaH_2 prior to use. THF, diethyl ether, and toluene used in syntheses were distilled over Na (with benzophenone as an indicator) and transferred via syringe to avoid contact with air. Reagent grade CH_2Cl_2 was distilled prior to use as a reaction solvent. All other solvents were spec. or HPLC grade and used as received. HRMS measurements employed EI ionization and a magnetic sector mass analyzer.

Synthesis Procedures. *2-Phenyl-3-naphthol (**10**).*[18] A solution of 3-bromo-2-methoxynaphthalene (2.00 g, 8.4 mmol) in toluene (50 mL) was stirred and mixed with solutions of phenylboronic acid (1.23 g, 10 mmol) in ethanol (50 mL) and potassium carbonate (5.05 g) in water (50 mL). This resulting mixture was stirred and bubbled with Ar for 10 min. To the purged solution was added $Pd(PPh_3)_4$ (0.21 mol, 2.5 mol %), and the mixture was brought to reflux for 48 h under a positive pressure of argon. Once cool, the reaction mixture was diluted with dichloromethane (100 mL) and washed with 0.1 M sodium hydroxide solution (2 × 100 mL). The organic layer was dried ($MgSO_4$), and the solvent was removed under reduced pressure. The resulting oil (3-phenyl-2-methoxynaphthalene was dissolved in dichloromethane (25 mL) and was added dropwise to a stirring solution of BBr_3 (10 mmol in 80 mL of dichloromethane) in an ice bath under an argon atmosphere over a period of 10 min. The mixture was then removed from the ice bath and allowed to warm to room temperature and continue to stir for 3 h. The reaction was quenched by the addition of 100 mL of water. The organic layer was dried ($MgSO_4$), and the solvent was removed under reduced pressure. The resulting solid was recrystallized from heptanes to give **10**, a white solid (1.22 g, 66% from 3-bromo-2-methoxynaphthalene) as the final product. Spectroscopic data for **10** matched data previously reported for this compound.[18]

*1-Phenyl-2-methoxynaphthalene (**16**).*[19] A solution of 1-bromo-2-methoxynaphthalene (2.0 g, 8.4 mmol) and $Pd(PPh_3)_4$ (0.25 g, 0.21 mol, 2.5 mol %) in 50 mL toluene was stirred under a N_2 atmosphere. To this was added a solution of phenylboronic acid (1.22 g, 10 mmol) in 50 mL ethanol, and a solution of K_2CO_3 (5.0 g) in 50 mL water. The mixture was brought to reflux for 20 h, and allowed to cool to room temperature. The solution was filtered through a Celite plug and diluted with 100 mL of CH_2Cl_2, and washed with 2 × 100 mL of 0.1 M NaOH, and with 100 mL of water. The resulting solution was dried over $MgSO_4$, and the solvent was removed under vacuum. The crude product was recrystallized twice from hot 95% ethanol to give white crystals of **16** (1.26 g, 49%). ^{1}H NMR (500 MHz, $CDCl_3$) δ 7.88 (d, 1H, J = 7 Hz), 7.82 (m, 1H), 7.49 (m, 3H), 7.42 (ddd, J = 7.6, 7.3, 1.5), 7.37 (m, 3H), 7.33 (m, 2H), 3.83 (s, 3H). ^{13}C NMR (125 MHz, $CDCl_3$) δ 153.7, 136.4, 133.6, 131.0, 129.1, 129.0, 128.1, 127.8, 127.1, 126.3, 125.4, 125.3, 123.3, 113.9, 56.8. HRMS calcd. for $C_{17}H_{14}O$: 234.1045; observed 234.1045. NMR data are consistent with those previously reported.[19]

*1-Phenyl-2-naphthol (**11**).*[20] To a stirring solution of BBr_3 (1 M in CH_2Cl_2) (10 mL, 10 mmol) in CH_2Cl_2 (50 mL) under N_2 in an ice bath was added dropwise a solution of **16** (0.50 g, 2.1 mmol) in CH_2Cl_2 (30 mL) over a period of 30 min. The mixture was allowed to warm to room temperature as it was stirred for 2 h. The reaction was quenched with 100 mL of 10% HCl, and the organic layer was removed and washed with 2 × 100 mL of water. Solid residue was recrystallized from hot lingroins to give 0.18 g (39%) of **11** as white crystals. ^{1}H NMR (500 MHz, acetone-d_6) δ 8.01 (s, 1H, exchanges with D_2O), 7.82 (dd, 2H, J = 8.1, 7.2 Hz), 7.51 (m, 2H), 7.42 (ddd, 1H, J = 7.2, 7.5, 1.4 Hz), 7.37 (m, 3H), 7.24−7.33 (m, 3H). HRMS calcd. for $C_{16}H_{12}O$: 220.0888; observed 220.0885. The NMR data are consistent with those previously reported.[20]

*1-(2′-Methoxyphenyl)naphthalene (**17**).*[21] A solution of 2-bromoanisole (2.6 mL, 4.1 g, 22 mmol) and $Pd(PPh_3)_4$ (0.25 g, 0.21 mol, 1 mol %) in 50 mL of toluene was stirred under a N_2 atmosphere. To this was added a solution of 1-naphthaleneboronic acid (4.0 g, 23.3 mmol) in 50 mL of ethanol, and a solution of K_2CO_3 (10.0 g) in 50 mL of water. The mixture was brought to reflux for 20 h, and allowed to cool to room temperature. The solution was filtered through a Celite plug and diluted with 100 mL of CH_2Cl_2, and washed with 2 × 100 mL of 1 M NaOH, and with 100 mL of water. The resulting solution was dried over $MgSO_4$, and the solvent was removed under vacuum. The crude product was recrystallized from hot methanol to give white crystals

DOI: 10.1021/acs.joc.5b01580
J. Org. Chem. 2015, 80, 11281−11293

of **17** (3.95 g, 78%). ^{1}H NMR (300 MHz, $CDCl_3$) δ 7.87 (d, 1H, J = 7.8 Hz), 7.84 (d, 1H, J = 7.9), 7.58−7.33 (m, 6H), 7.27 (dd, 1H, J = 7.5, 1.7 Hz), 7.09−7.02 (m, 2H), 3.68 (s, 3H). ^{13}C NMR (125 MHz, $CDCl_3$) δ 157.5, 137.2, 133.7, 132.4, 132.2, 129.8, 129.2, 128.3, 127.9, 127.5, 126.7, 125.9, 125.8, 125.6, 120.8, 111.2, 55.8. HRMS calcd. for $C_{17}H_{14}O$: 234.1045; observed 234.1046. The NMR data matches those previously reported.[21]

*1-(2′-Hydroxyphenyl)naphthalene (**12**).*[22] To a stirring solution of BBr_3 (1 M in CH_2Cl_2) (20 mL, 20 mmol) in CH_2Cl_2 (50 mL) under N_2 in an ice bath was added dropwise a solution of **17** (2.0 g, 8.5 mmol) in CH_2Cl_2 (50 mL) over a period of 30 min. The mixture was allowed to warm to room temperature as it was stirred for 2 h. The reaction was quenched with 100 mL of 10% HCl and diluted with 50 mL of CH_2Cl_2, and the organic layer was removed and washed with 2 × 150 mL of water (brine was added to aid in separation). The organic layer was dried over $MgSO_4$, and solvent was removed under vacuum to afford a deep orange oil. The oil was purified by bulb to bulb distillation to give **12** as a colorless oil (1.54 g, 82%). ^{1}H NMR (500 MHz, acetone-d_6) δ 7.98 (br s, 1H, exchanges with D_2O), 7.94 (ddd, 1H, J = 8.1, 1.7, 1.0 Hz), 7.91 (d, 1H, J = 8.1 Hz), 7.67−7.62 (m, 1H), 7.55 (dd, 1H, J = 8.1, 8.1 Hz), 7.51−7.47 (m, 1H), 7.44−7.40 (m, 2H), 7.31 (ddd, 1H, J = 8.0, 7.7, 1.8 Hz), 7.22 (dd, 1H, J = 7.7, 1.8 Hz), 7.08 (dd, 1H, J = 8.1, 1.2 Hz), 7.00, dd, 1H, J = 7.7, 7.3, 1.2 Hz). ^{13}C NMR δ 155.8, 137.9, 134.8, 133.3, 132.6, 130.0, 129.0, 128.6, 128.5, 128.4, 127.3, 126.63, 126.57, 126.4, 120.6, 116.78. HRMS calcd. for $C_{16}H_{12}O$: 220.0888; observed 220.0886. The NMR data are similar to those reported previously for this compound, although the previously reported spectra were recorded in a different solvent.[22]

*1-(1′-Naphthyl)-2-methoxynaphthalene (**18**).*[19] A solution of 1-bromo-2-methoxynaphthalene (3.0 g, 12.65 mmol), $Pd(PPh_3)_4$ (0.75 g, 0.63 mmol), DME (100 mL), 1-naphthaleneboronic acid (2.58 g, 15 mmol), and 1 M $NaHCO_{3(aq)}$ (75 mL) was stirred under N_2 and brought to reflux for 45 h, and allowed to cool. The solution was filtered through a Celite plug and diluted with 100 mL of CH_2Cl_2, and washed with 2 × 100 mL of 1 M NaOH, and with 100 mL of water. The resulting solution was dried over $MgSO_4$, and the solvent was removed under vacuum to afford a thick deep orange oil. NMR of the crude material indicated ∼75% conversion of the starting bromide. The oil was purified by bulb to bulb distillation, with the fraction that was collected between 90 and 165 °C kept. This fraction was recrystallized from hot methanol to give **18** as white crystals (1.75 g, 49%). ^{1}H NMR (500 MHz, $CDCl_3$) δ 7.98 (d, 1H, J = 8 Hz), 7.95 (m, 2H), 7.87 (d, 1H, J = 8 Hz), 7.61 (dd, 1H, J = 8, 8 Hz), 7.42−7.46 (m, 3H), 7.29−7.34 (m, 3H), 7.22 (ddd, 1H, J = 8, 8, 1 Hz), 7.16 (d, 1H, J = 8 Hz), 3.56 (s, 3H). ^{13}C NMR (125 MHz, $CDCl_3$) δ 154.8, 134.8, 134.5, 133.9, 133.2, 129.7, 129.2, 128.7, 128.4, 128.1, 128.0, 128.0, 126.6, 126.4, 126.2, 126.0, 125.8, 125.7, 123.8, 114.1, 57.0. HRMS calcd. for $C_{21}H_{16}O$: 284.1201; observed 284.1199. NMR data are consistent with those previously reported.[19]

*1-(1′-Naphthyl)-2-naphthol (**13**).*[23] To a stirring solution of BBr_3 (1 M in CH_2Cl_2) (15 mL, 15 mmol) in CH_2Cl_2 (50 mL) under N_2 in an ice bath was added dropwise a solution of **18** (1.0 g, 3.5 mmol) in CH_2Cl_2 (50 mL) over a period of 30 min. The mixture was allowed to warm to room temperature as it was stirred for 2 h. The reaction was quenched with 100 mL of water and diluted with 50 mL of CH_2Cl_2, and the organic layer was removed and washed with 2 × 200 mL of water (brine was added to aid in separation). The organic layer was dried over $MgSO_4$, and solvent was removed under vacuum to give **13** as a crude solid. The solid was recrystallized from methanol twice to give **13** in two crops as white crystals (0.60 and 0.15 g, 80%). ^{1}H NMR (500 MHz, $CDCl_3$) δ 8.02 (d, 1H, J = 8.3 Hz), 7.96 (d, 1H, J = 8.2 Hz), 7.89 (d, 1H, J = 8.9 Hz), 7.85 (dt, 1H, J = 8.1, 1.3 Hz), 7.65 (dd, 1H, J = 8.2, 8.1 Hz), 7.53 (dd, 1H, J = 6.8, 1.2 Hz), 7.52−7.50 (m, 1H), 7.37 (dd, 1H, J = 8.4, 0.6 Hz), 7.31−7.35 (m, 3H), 7.24−7.21 (m, 1H), 7.09 (dt, J = 8.4, 1.3 Hz). ^{13}C NMR (125 MHz, $CDCl_3$) δ 151.0, 134.1, 133.9, 132.8, 131.4, 129.8, 129.6, 129.2, 128.9, 128.4, 128.0, 127.7, 126.8, 126.46, 126.45, 125.9, 124.9, 123.3, 118.8, 117.4. HRMS calcd. for $C_{20}H_{14}O$: 270.1045; observed 270.1043. NMR data are consistent with those previously reported for the R enantiomer of **13**.[23]

*9-(2-Methoxyphenyl)phenanthrene (**19**).*[24] A mixture of 500 mg (1.95 mmol) of 9-bromophenanthrene and 325 mg (2.14 mmol) of 2-methoxyphenylboronic acid was dissolved in DME in a 100 mL round-bottom flask. To the reaction mixture was added 2 equiv of 2 M aqueous K_2CO_3, and the solution was purged with N_2 for 20 min. To the reaction mixture was added 112 mg (0.107 mmol) of $Pd(PPh_3)_4$, and the solution was purged again with N_2. The reaction mixture was heated at reflux for 18 h under a N_2 atmosphere. The reaction mixture was then cooled to room temperature and extracted with ethyl acetate (×3). The combined extracts was washed with brine and then dried over anhydrous $MgSO_4$. Filtration and concentration under reduced pressure afforded the crude product **19**. Purification was achieved by flash chromatography on silica gel (EtOAc/hexane gradient, 0% to 5%) to furnish **19** as a colorless oil (457 mg, 87%). ^{1}H NMR (500 MHz, $CDCl_3$) δ 8.74 (d, 1 H, J = 8.3 Hz), 8.71 (d, 1 H, J = 8.3 Hz), 7.87 (d, 1 H, J = 7.7 Hz), 7.66 (s, 1 H),7.65−7.56 (m, 4 H), 7.49−7.43 (m, 2 H), 7.34 (dd, 1 H, J = 7.4, 2.0 Hz), 7.10 (td, 1 H, J = 7.4, 1.1 Hz), 7.06 (dd, 1 H, J = 8.3, 0.9 Hz), 3.68 (s, 3 H); ^{13}C NMR (125 MHz, $CDCl_3$) δ 157.7, 136.1, 132.1, 132.0, 131.7, 130.4, 130.38, 129.9, 129.4, 128.9, 128.0, 127.4, 126.8, 126.7, 126.5, 126.4, 122.9, 122.8, 120.9, 111.2, 55.8. Spectroscopic data are consistent with those previously reported for this compound.[24]

*9-(2′-Hydroxyphenyl)phenanthrene (**14**).*[25] To a solution of the methoxy compound **19** (370 mg, 1.30 mmol in 10 mL of CH_2Cl_2) at 0 °C was added 3 equiv of BBr_3 (1 M in CH_2Cl_2) dropwise under N_2. The ice bath was removed, and the reaction mixture was stirred at room temperature for an additional 2 h under N_2. The reaction was quenched by CH_3OH and stirred for 10 min. Following addition of water, the mixture was extracted twice with CH_2Cl_2 and the combined extracts were dried over anhydrous $MgSO_4$. Filtration and concentration under reduced pressure afforded the crude product. The crude product was then purified by flash chromatography on silica gel (EtOAc/hexane gradient, 0% to 20%) and further purified by recrystallization from methylene chloride and *n*-hexanes to provide **14** as an off-white solid (341 mg, 97%). ^{1}H NMR (500 MHz, $CDCl_3$) δ 8.78 (d, 1 H, J = 8.8 Hz), 8.74 (d, 1 H, J = 8.3 Hz), 7.89 (dd, 1 H, J = 7.7, 1.2 Hz), 7.77 (s, 1 H), 7.73−7.68 (m, 3 H), 7.64 (td, 1 H, J = 7.6, 1.2 Hz), 7.54 (td, 1 H, J = 7.6, 1.2 Hz), 7.41−7.37 (m, 1 H), 7.32 (dd, 1 H, J = 7.6, 1.6 Hz), 7.10−7.06 (m, 2 H), 4.84 (s, 1 H, OH); ^{13}C NMR (125 MHz, $CDCl_3$) δ 153.6, 132.8, 131.6, 131.5, 131.1, 131.0, 130.7, 129.9, 129.4, 129.0, 127.5, 127.4, 127.35, 127.3, 126.8, 126.5, 123.3, 122.9, 120.9, 115.9. HRMS, calcd for $C_{20}H_{14}O$: 270.10447; Found 270.10427. NMR data are consistent with those previously reported for this compound.[25]

Product Studies. *General.* A solution of the substrate (∼10^{-4} to 10^{-3} M, 40−100 mL total) was added to a quartz vessel with a cooling finger (∼15 °C) and was purged with argon gas for 10 min prior to and continuously during irradiation in a Rayonet RPR 100 photochemical reactor using 254, 300, or 350 nm lamps. Photolysis times ranged from 3 to 120 min, depending on the conversion desired, the efficiency of the reaction, and the concentration of the sample. After photolysis, aqueous samples were worked up by extraction with CH_2Cl_2 after addition of aq. NaCl. Direct evaporation of the organic solvent was used when samples were irradiated in wholly organic solvents. Separation of the photolysate was carried out using preparatory-scale TLC when needed.

*Photolysis of **12** in 1:9 H_2O−CH_3CN.* Irradiation of **12** dissolved in 1:9 H_2O−CH_3CN (λ_{ex} 300 nm, ∼10^{-3} M, 16 lamps, 20 min, argon purged) gave **20** in 80% yield, which was separated from the unreacted starting material on silica gel (eluent 1:9 diethyl ether−hexanes). ^{1}H NMR (500 MHz, $CDCl_3$) δ 7.76 (dd, 1H, J = 7.7, 1.7 Hz), 7.56 (d, 1H, J = 7.7 Hz), 7.34 (t, 1H, J = 7.7 Hz), 7.24 (ddd, 1H, J = 7.9, 7.7, 1.4 Hz), 7.17 (d, 1H, J = 7.6 Hz), 7.08−7.03 (m, 2H), 6.27−6.19 (m, 2H), 5.39−5.36 (m, 1H), 3.49−3.37 (m, 2H). ^{13}C NMR (125 MHz, $CDCl_3$) δ 155.6, 131.9, 130.4, 129.3, 128.3, 128.0, 127.3, 127.1, 125.4, 123.9, 123.6, 122.2, 120.2, 117.5, 69.6, 29.6.

*Photolysis of **12** in 1:1 D_2O−CH_3CN.* Irradiation of **12** in 1:1 D_2O−CH_3CN (∼10^{-3} M, argon purged, λ_{ex} 300 nm, 16 lamps, 20 min) gave **20**-7′*D* in 23% yield, **12**-2′*D* in 19% yield, and small amounts of other minor products that were not isolated.

*Photolysis of **13**.* Irradiation of 73 mg of **13** dissolved in 1:1 H_2O−CH_3CN (λ_{ex} 300 nm, 16 lamps, 40 min, argon purged) gave **21**, which was separated from the unreacted starting material on silica gel (eluent 15% diethyl ether in hexanes, R_f ∼ 0.7). ^{1}H NMR (500 MHz,

DOI: 10.1021/acs.joc.5b01580
J. Org. Chem. 2015, 80, 11281−11293

$CDCl_3$) δ 8.56 (d, 1H, 8.5 Hz), 7.89 (d, 1H, J = 7.7 Hz), 7.84 (d, 1H, J = 8.3 Hz), 7.73 (d, 1H, J = 8.8 HZ), 7.53 (ddd, 1H, J = 8.4, 6.8, 1.3 Hz), 7.41 (d, 1H, J = 7.8 Hz), 7.39 (d, 1H, 7.7 Hz), 7.27 (d, 1H, J = 8.8 Hz), 7.24 (d, 1H, J = 7.7 Hz), 6.34−6.24 (m, 2H), 5.24−5.20 (m, 1H), 3.54−3.51 (m, 1H). ^{13}C NMR (125 MHz, $CDCl_3$) δ 155.0, 131.8, 130.6, 130.5, 129.9, 129.5, 128.8, 128.1, 127.8, 126.8, 126.7, 124.9, 124.4, 124.3, 123.9, 118.3, 116.73, 116.65, 69.9, 29.6. HRMS calcd. for $C_{20}H_{14}O$: 270.1045; observed 270.1046.

*Photolysis of **13** in 1:9 D_2O−CH_3CN.* Irradiation of 13 mg of **13** dissolved in 1:9 D_2O−CH_3CN (λ_{ex} 300 nm, ~10^{-3} M, 16 lamps, 4 min, argon purged) gave **21**-7′*D* in 26% yield, and **13**-2′*D* in 27% yield, as determined by 500 MHz ^{1}H NMR.

*Photolysis of **10**, **11**, **16**−**19**.* Solutions of each of **10**, **11**, **16**, **17**, **18**, and **19** were prepared (1:1 D_2O−CH_3CN), and each was irradiated for 60 min. No deuterium incorporation could be observed by ^{1}H NMR (500 MHz) for any of these derivatives, and no new products were formed.

*Photolysis of **14** in 1:1 H_2O−CH_3CN.* A solution of 30 mg of **14** was dissolved in 100 mL of 1:1 H_2O−CH_3CN and irradiated at 300 nm for 3 h. Purification was achieved by preparative TLC plate to afford 10% yield of **24** as an off-white solid. ^{1}H NMR (500 MHz, CDCl3) δ 8.50−8.48 (m, 1 H), 8.19 (d, 1 H, J = 8.1 Hz), 7.99 (dd, 1 H, J = 7.6, 1.4 Hz), 7.84 (s, 1 H), 7.83−7.81 (m, 1 H), 7.57−7.53 (m, 3 H), 7.31 (td, 1 H, J = 7.8, 1.4 Hz), 7.17−7.12 (m, 3 H); ^{13}C NMR (125 MHz, $CDCl_3$) δ 151.9 151.3, 133.0, 132.2, 130.1, 129.4, 128.8, 128.1, 127.6, 126.4, 124.9, 123.7, 123.2, 120.5, 119.4, 117.6, 116.2, 114.4, 111.3; HRMS, calcd for $C_{20}H_{12}O$: 268.08820; Found 268.08868.

*Photolysis of **14** in 1:1 D_2O−CH_3CN.* A solution of 50 mg of **14** was dissolved in 150 mL of 1:1 D_2O−CH_3CN and irradiated at 300 nm for 5 h. Purification was achieved by preparative TLC plate to afford a mixture of **14** and **24**, along with a trace amount of **25**. Product **14** isolated from the photolysate showed an 84% decrease in the integration of the singlet peak at 7.77 ppm assigned to the proton at the 10′-position of the phenanthrene ring (Figure 1). The isolated cyclized product **24** also showed deuterium exchange at two positions, 10′- and 4′-positions, which were confirmed by the 72% and 58% decreased integration at peaks 8.19 and 7.84 ppm, respectively. Isolation of the trace amount of **25** was unsuccessful due to its thermal instability that probably causes it to slowly transform into **24**. The structure for **25** we propose is based on the ^{1}H NMR spectrum of the crude photolysate that shows a doublet of doublets at 6.31 ppm with a distinct olefin coupling constant of 11 MHz and a broad peak at 3.60 ppm attributable to a methylene group with one hydrogen and one deuterium atom.

*Photolysis of **14** in 1:2:5 CH_3OH−H_2O−CH_3CN.* A solution of 25 mg of **14** was dissolved in 80 mL of 1:2:5 CH_3OH−H_2O−CH_3CN and irradiated at 350 nm for 18 h. Purification was achieved by preparative TLC plate to afford 70% yield of methyl ether **22** and 4% yield of **24**. Compound **22**: ^{1}H NMR (500 MHz, CDCl3) δ 8.94 (s, 1 H, OH), 7.91 (d, 1 H, J = 7.8 Hz), 7.83 (d, 1 H, J = 7.8), 7.46−7.43 (m, 1 H), 7.34 (dt, 1 H, J = 8.2, 1.8 Hz), 7.28−7.23 (m, 2 H), 7.24−7.19 (m, 3 H), 6.95 (dd, 1 H, J = 8.2, 1.2 Hz), 6.85 (dd, 1 H, J = 7.9, 1.6 Hz), 6.74 (dt, 1 H, J = 7.6, 1.6 Hz), 4.59 (d, 1 H, J = 15.6), 4.49 (d, 1 H, J = 15.6), 3.18 (s, 3 H, OMe); ^{13}C NMR (125 MHz, $CDCl_3$) δ 156.9, 135.4, 135.2, 133.8, 133.2, 129.8, 129.5, 128.9, 128.3, 128.2, 128.1, 127.7, 125.5, 124.6, 123.7, 119.8, 117.7, 83.9, 52.2, 38.6.

Quantum Yields. Quantum yields were measured for the formation of photoproducts from **12**, **13**, and **14**. The deuterium exchange reaction at the 2′-position of 2-phenylphenol (Φ = 0.084) was used as a secondary reference standard.[4] Photoreactions were carried out to low conversion (<15%), and the photolysate was analyzed by ^{1}H NMR. The reported values were determined from the average of four trials.

The quantum yields for formation of **12**-2′*D* and **20**-7′*D* from **12** in 1:9 D_2O−CH_3CN were measured to be 0.14 and 0.20, respectively. The quantum yields for formation of **13**-2′*D* and **21**-7′*D* from **13** in 1:9 D_2O−CH_3CN were both measured to be 0.11. The quantum yields for formation of **14**-10′*D* and **24** (total of di- and monodeuterated) in 1:1 D_2O−CH_3CN were 0.18 and 0.005, respectively. The quantum yields for formation of **14**-10′*D* increased when the solvent was changed to 1:99 D_2O−CH_3CN. All values are estimated to have errors of ±10% of the quoted value.

UV−vis Studies. Solutions were prepared in 1 cm quartz cuvettes by filling with 3 mL of the appropriate solvent and spiking with 1−5 μL of a concentrated solution of the substrate in acetonitrile to get the desired OD. Final concentrations are 10^{-6} to 10^{-5} M. Cuvettes were then bubbled with argon or nitrogen for 5−10 min to remove dissolved oxygen, and capped tightly. Irradiations of cuvettes were carried out directly in a Rayonet RPR-100 photochemical reactor with cooling achieved with a fan. Traces were recorded after regular irradiation time intervals.

Steady State Fluorescence and Lifetime Measurements. Solutions for steady state fluorescence and lifetime measurements were prepared in 1 cm quartz cuvettes by adding 3 mL of the appropriate solvent and spiking with a concentrated stock solution of the substrate in CH_3CN. Spike volumes were adjusted to give OD = 0.1 at the excitation wavelength and were typically in the 1−5 μL range. Solutions were then bubbled with argon or nitrogen gas for 5−10 min and tightly capped prior to measurement.

Fluorescence quantum yields were determined by comparing the integrated emission bands of a standard with those of the desired compound, according to the following equation

$$\Phi_u = \Phi_s(A_s F_u \eta_u^2 / A_u F_s \eta_s^2)$$

where Φ_u and Φ_s refer to the fluorescence quantum yields of the unknown and standard; A_u and A_s refer to the absorbance of the unknown and standard sample; F_u and F_s refer to the area of the total area of the integrated fluorescence bands of the unknown and standard; and η_u and η_s are the refractive indices of the solvent containing the unknown and standard.

Fluorescence lifetimes were measured by a single photon counting PTI LS-1 instrument with a low pressure H_2 arc lamp as the excitation source. Software supplied with the instrument was used to collect data, deconvolute the signals from the lamp and the sample, and to fit the data. All decays measured were first-order.

Laser Flash Photolysis (LFP). LFP studies were carried out at the University of Victoria LFP facility with excitation achieved by either a Spectra Physics YAG laser (GCR-11, λ_{ex} = 266 or 355 nm) or a Lumonics excimer laser (Model EX-510, λ_{ex} = 308 nm). Photon energies were kept below 25 mJ/pulse by use of neutral density filters (for excimer laser) or attenuation of power (for YAG laser). Solutions used for collecting LFP spectra were flowed from a chamber containing 50−100 mL of solution containing the substrate with OD = 0.3 at λ_{ex}. This solution was bubbled 10 min prior and continuously during the experiment, and was flowed into a 7 mm × 7 mm quartz cell at flow rates at ~1 mL per minute. LFP quenching experiments were carried out in 7 mm × 7 mm quartz cells containing solution with substrate at OD = 0.3 at λ_{ex}. These solutions are bubbled with nitrogen gas for 5−10 min prior to study. Spectra were generated by plotting the absorbance value at a fixed time after laser excitation for a given monitoring wavelength, and repeating for other monitoring wavelengths at 10 or 20 nm increments across the UV−visible range (260−800 nm). Data points plotted are the average of 8−10 shots at each monitoring wavelength. Decay data were obtained by measuring 500 absorbance points at equivalent time intervals within a chosen time scale. Available time scales ranged from 50 ns to 1 ms. Fits were performed on the average of 8−20 decays recorded in this fashion.

■ ASSOCIATED CONTENT

Supporting Information

The Supporting Information is available free of charge on the ACS Publications website at DOI: 10.1021/acs.joc.5b01580.

Copies of the ^{1}H and ^{13}C NMR spectra, and UV−vis, fluorescence, and LFP data (PDF)

■ AUTHOR INFORMATION

Corresponding Authors

*Fax: +1 902 585-1114. Tel: +1 902 585-1009. E-mail: mlukeman@acadiau.ca (M.L.).

*E-mail: lily.wang@pharmaster.ca (Y.-H.W.).

DOI: 10.1021/acs.joc.5b01580
J. Org. Chem. 2015, 80, 11281−11293

Notes

The authors declare no competing financial interest.

■ ACKNOWLEDGMENTS

We are grateful for the continued support by the Natural Sciences and Engineering Research Council of Canada (NSERC). H.S. thanks Acadia University and the Nova Scotia Strategic Cooperative Education Incentive (SCEI) for financial support.

■ REFERENCES

(1) Part of this work has appeared in preliminary form: Lukeman, M.; Wan, P. *J. Am. Chem. Soc.* **2003**, *125*, 1164.
(2) (a) Ormson, S. M.; Brown, R. G. *Prog. React. Kinet.* **1994**, *19*, 45. (b) Le Gourrierec, D.; Ormson, S. M.; Brown, R. G. *Prog. React. Kinet.* **1994**, *19*, 211. (c) Formosinho, S. J.; Arnaut, L. G. *J. Photochem. Photobiol., A* **1993**, *75*, 21.
(3) (a) Isaks, M.; Yates, K.; Kalanderopoulos, P. *J. Am. Chem. Soc.* **1984**, *106*, 2728. (b) Kalanderopoulos, P.; Yates, K. *J. Am. Chem. Soc.* **1986**, *108*, 6290. (c) Lukeman, M. In *Quinone Methides*; Rokita, S. E., Ed.; Wiley: New York, 2009; Chapter 1. (d) Basarić, N.; Mlinarić-Majerski, K.; Kralj, M. *Curr. Org. Chem.* **2014**, *18*, 3. (e) Doria, F.; Percivalle, C.; Freccero, M. *J. Org. Chem.* **2012**, *77*, 3615.
(4) Lukeman, M.; Wan, P. *J. Am. Chem. Soc.* **2002**, *124*, 9458.
(5) Lukeman, M.; Veale, D.; Wan, P.; Munasinghe, V. R. N.; Corrie, J. E. T. *Can. J. Chem.* **2004**, *82*, 240.
(6) Kasha, M. *J. Chem. Soc., Faraday Trans. 2* **1986**, *82*, 2379.
(7) Flegel, M.; Lukeman, M.; Huck, L.; Wan, P. *J. Am. Chem. Soc.* **2004**, *126*, 7890.
(8) Flegel, M.; Lukeman, M.; Wan, P. *Can. J. Chem.* **2008**, *86*, 161.
(9) (a) Wang, Y.-H.; Wan, P. *Photochem. Photobiol. Sci.* **2013**, *12*, 1571. (b) Wang, Y.-H.; Wan, P. *Photochem. Photobiol. Sci.* **2011**, *10*, 1934.
(10) Basarić, N.; Došlić, N.; Ivković, J.; Wang, Y.-H.; Mališ, M.; Wan, P. *Chem. - Eur. J.* **2012**, *18*, 10617.
(11) Basarić, N.; Došlić, N.; Ivković, J.; Wang, Y.-H.; Veljković, J.; Mlinarić-Majerski, K.; Wan, P. *J. Org. Chem.* **2013**, *78*, 1811.
(12) Niimi, K.; Mori, H.; Miyazaki, E.; Osaka, I.; Kakizoe, H.; Takimiya, K.; Adachi, C. *Chem. Commun.* **2012**, *48*, 5892.
(13) This type of intramolecular ground state interaction between phenols and aromatic π-systems has been investigated in detail, for example: (a) Tarakeshwar, P.; Choi, H. S.; Kim, K. S. *J. Am. Chem. Soc.* **2001**, *123*, 3323. (b) Ōki, M.; Iwamura, H. *J. Am. Chem. Soc.* **1967**, *89*, 576. (c) Schaefer, T.; Wildman, T. A.; Sebastian, R.; McKinnon, D. M. *Can. J. Chem.* **1984**, *62*, 2692.
(14) (a) Arumugam, S.; Popik, V. V. *J. Am. Chem. Soc.* **2009**, *131*, 11892. (b) Arumugam, S.; Popik, V. V. *J. Am. Chem. Soc.* **2011**, *133*, 5573. (c) Colloredo-Mels, S.; Doria, F.; Verga, D.; Freccero, M. *J. Org. Chem.* **2006**, *71*, 3889. (d) Verga, D.; Nadai, M.; Doria, F.; Percivalle, C.; Di Antonio, M.; Palumbo, M.; Richter, S. N.; Freccero, M. *J. Am. Chem. Soc.* **2010**, *132*, 14625.
(15) Ma, J.; Zhang, X.; Basarić, N.; Wan, P.; Phillips, D. L. *Phys. Chem. Chem. Phys.* **2015**, *17*, 9205−9211.
(16) Webb, S. P.; Philips, L. A.; Yeh, S. W.; Tolbert, L. M.; Clark, J. H. *J. Phys. Chem.* **1986**, *90*, 5154.
(17) Kulikov, A.; Arumugam, S.; Popik, V. V. *J. Org. Chem.* **2008**, *73*, 7611−7615.
(18) Madhushaw, R. J.; Lin, M.-Y.; Sohel, S.; M, A.; Liu, R.-S. *J. Am. Chem. Soc.* **2004**, *126*, 6895−6899.
(19) Tu, T.; Sun, Z.; Fang, W.; Xu, M.; Zhou, Y. *Org. Lett.* **2012**, *14*, 4250−4253.
(20) Rasmussen, L. K.; Begtrup, M.; Ruhland, T. *J. Org. Chem.* **2004**, *69*, 6890−6893.
(21) Saha, D.; Ghosh, R.; Dutta, R.; Mandal, A. K.; Sarkar, A. *J. Organomet. Chem.* **2015**, *776*, 89−97.
(22) Rastogi, S. K.; Medellin, D. C.; Kornienko, A. *Org. Biomol. Chem.* **2014**, *12*, 410−413.
(23) Ma, G.; Deng, J.; Sibi, M. P. *Angew. Chem., Int. Ed.* **2014**, *53*, 11818−11821.
(24) Terao, Y.; Wakui, H.; Nomoto, M.; Satoh, T.; Miura, M.; Nomura, M. *J. Org. Chem.* **2003**, *68*, 5236−5243.
(25) Rice, J. E.; Cai, Z.-W. *J. Org. Chem.* **1993**, *58*, 1415−1424.

DOI: 10.1021/acs.joc.5b01580
J. Org. Chem. 2015, 80, 11281−11293